Pergamon

Phys. Chem. Earth (A), Vol. 24, No. 1, pp. 19–25, 1999

1464-1895/99/$—see front matter

PII: S1464-1895(98)00005-2

Gravity Field Recovery from Airborne Gradiometer Data Using Collaction and Taking Into Account Correlated Errors

D. Arabelos[1] and C. C. Tscherning[2]

[1]Department of Geodesy and Surveying, University of Thessaloniki, GR-540 06 Thessaloniki, Greece
[2]Department of Geophysics, University of Copenhagen, Juliane Maries Vej 30, DK-2100 Copenhagen Oe, Denmark

Received 4 May 1998; revised 7 September 1998; accepted 10 September 1998

Abstract. Least squares collocation is a very comprehensive method for gravity field modelling, since it may use known noise characteristics of the data. In many earlier applications the errors affecting the data were considered uncorrelated, mainly due to the difficulty in estimating the systematic character of such kind of errors. In this study, error covariance functions of airborne gravity gradiometer data are estimated by comparing model covariance functions with empirical covariance functions of the gravity gradiometer data. The model covariance functions were estimated from accurate surface gravity data and continuated upward to the height of the airborne measurements using the covariance propagation law. The estimated error covariance functions were modeled as finite ones and used as an additional information for the prediction of gravity anomalies from gravity gradiometer data. The assessment of the prediction results was made by comparing the gravity values predicted from the airborne gradient data and showed up to 25% improvement compared to not using correlated errors.

1 Introduction

In gravity field approximation by Least Squares Collocation (LSC) the well known formula is used (e.g. Moritz , 1980)

$$s_{res} = \mathbf{C}_{res,x}^{T}(\mathbf{C} + \mathbf{D})^{-1}\mathbf{x}_{res}, \qquad (1)$$

where:

s_{res} is the wanted residual signal with respect to a geopotential model,

$\mathbf{C}_{res,x}^{T}$ is the vector of covariances between s_{res} and the residual observation $\mathbf{x}_{res}$,

$\mathbf{C}$ is the matrix of covariances between the residual observations $\mathbf{x}_{res}$, and

$\mathbf{D}$ is the matrix of the error covariances between the residual observations $\mathbf{x}_{res}$.

Correspondence to: D. Arabelos

In many geodetic applications the errors of the observations are considered as uncorrelated, so that $\mathbf{D}$ is a diagonal matrix of the observation noise. However, the assumption of uncorrelated errors is a convenient compromise, since the estimation of error covariance functions is a rather difficult task. On the other hand, the prediction of quantities related to the gravity field from observations affected by systematic errors leads to prediction results of lower accuracy, when the systematic errors are ignored (e.g. Arabelos and Tziavos, 1992).

In the present paper a numerical verification of this statement was attempted according to the following procedure: Point gravity anomalies from airborne gravity gradient data were predicted by LSC. In a first stage the prediction was made assuming uncorrelated errors for the gravity gradient data. Then the prediction was repeated at the same points but taking into account the correlated errors. The predicted gravity anomalies from these experiments were compared with point gravity anomalies at the ground and the comparison showed the importance of taking systematic errors into account.

The test field of our experiment was in Texas/Oklahoma area where the airborne Gravity Gradiometer Survey System (GGSS) took the first test flight in the spring of 1987 (see Brzezowski et al., 1988a,b; Gleason, 1988; Vasco, 1989; Wang, 1989).

In an earlier paper (Arabelos and Tziavos , 1992) the same data set was used in a successful attempt to recover the gravity field from airborne gravity gradient observations. These results were not used in the present paper, since the geopotential model EGM96 (Lemoine et al. , 1996) was used instead of OSU89B and RTM reductions (Forsberg and Tscherning, 1981) were additionally used to smooth further the gravity field in the test area. However, the experience concerning the gravity gradiometer data gained by the 1992 paper was very useful in the present paper.

For the second- order derivatives of the anomalous potential T with respect to a local (x, y, z) coordinate frame (East, North, Up) we use the following notation (see Arabelos and

Tscherning, 1990):

$$T_{zz} = \frac{\partial^2 T}{\partial z^2}, T_{zx} = \frac{\partial^2 T}{\partial zx}, T_{zy} = \frac{\partial^2 T}{\partial zy}, T_{xy} = \frac{\partial^2 T}{\partial xy}, \quad T_{xx} = \frac{\partial^2 T}{\partial xx}, T_{yy} = \frac{\partial^2 T}{\partial yy} \tag{2}$$

2 Data description and processing

2.1 DEM

A 30″ elevation model for the area bounded by $30^o \leq \varphi \leq 39^o, 254^o \leq \lambda \leq 268^o$ was made available to us by S. Kenyon (private communication, 1997). This very detailed DEM (see Fig. 1) was used to apply RTM reductions to gravity gradient data as well as to gravity data. From Fig. 1 it is evident that the topography in the test area ($33.75^o \leq \varphi \leq 34.75^o, 261^o \leq \lambda \leq 262^o$) is very smooth.

2.2 GGSS data

Arabelos and Tziavos (1992) give details about the problems related to the original data set produced by Bell Aerospace and the procedure followed in order to produce the final data subset that was distributed to the IAG SSG 3.111 members by C. Jekeli. This latter data subset included the six components of the gravity gradient tensor measured at 45,219 points along 19 tracks (with a 1 second resolution in time or approximately 111 meters in distance) oriented north-south (or south-north) and east-west (or west-east). The six gradients were referred to a local North-East-Down (NED) reference system using the transformation matrix given by Jekeli (1985). In order to be compatible to the reference system used by GEOCOL FORTRAN program (Tscherning, 1985) the gradient values were transformed from their NED system to an East-North-Up (ENU) system using the well known transformation matrices. The distribution of the gravity gradient data is shown in Fig. 1 The statistics of the six components of the original data is shown in Table 1, row 1.

The analysis in Arabelos and Tziavos (1992, section 2) showed that the data are very noisy. As an example, Fig. 2 is a plot of the original T_{zz} values along track No. 4. Taking into account the very dense distribution of the data along each track ($\cong$ 111 m) and the mean separation between the tracks ($\cong$ 5 km) a low pass gaussian filter was applied along each track using a filter width equal to 0.0333^o. The routine FILTER1D from the GMT package (Wessel and Smith, 1995) was used for this purpose. Fig. 3 shows the filtered T_{zz} values along track No. 4. It is evident that the filtered T_{zz} values of Fig. 3 are smooth compared to the original ones of Fig. 2. The statistics of the filtered data is shown in Table 1, row 2. Not only for T_{zz} but for all the six components of the gravity gradient tensor the decrease of the standard deviation (std) is considerable while the change of the mean value is negligible. The filtering process will make the errors of the gradients correlated if they are not already correlated.

Table 1. Statistics of the gravity gradient components before and after the reductions. The number of the original data is 45,219. After the filtering the number of the data is 44,250. Unit is EU = 10^{-9} sec^{-2}

	T_{zz}			
	Mean	Std	Min. value	Max. value
Original	-0.104	24.471	-112.285	103.448
Filtered	-0.135	21.250	-87.270	89.440
Filtered-EGM96	-0.841	20.015	-92.240	75.510
Filtered-EGM96 - RTM	-0.430	19.599	-92.986	81.027
	T_{yz}			
	Mean	Std	Min. value	Max. value
Original	0.059	18.576	-88.829	93.600
Filtered	0.053	15.780	-67.220	76.190
Filtered-EGM96	-1.201	14.870	-69.210	70.400
Filtered-EGM96 - RTM	-1.175	15.448	-82.191	69.698
	T_{xz}			
	Mean	Std	Min. value	Max. value
Original	0.143	19.423	-84.931	101.394
Filtered	0.117	17.147	-60.460	87.240
Filtered - EGM96	-1.517	16.590	-59.430	84.840
Filtered - EGM96 - RTM	-1.615	16.810	-60.392	79.276
	T_{xy}			
	Mean	Std	Min. value	Max. value
Original	-0.186	16.030	-101.173	102.221
Filtered	-0.275	13.202	-84.350	88.960
Filtered - EGM96	0.106	13.237	-72.590	90.530
Filtered - EGM96 - RTM	0.101	13.170	-71.031	88.280
	T_{yy}			
	Mean	Std	Min. value	Max. value
Original	-0.196	19.231	-79.729	98.675
Filtered	0.178	16.494	-93.570	61.830
Filtered - EGM96	0.728	16.003	-96.740	62.350
Filtered - EGM96 - RTM	0.466	16.138	-99.971	69.871
	T_{xx}			
	Mean	Std	Min. value	Max. value
Original	0.200	20.062	-112.644	93.234
Filtered	-0.043	15.886	-58.500	78.190
Filtered - EGM96	0.098	15.442	-56.260	81.330
Filtered - EGM96 - RTM	-0.051	15.631	-59.148	81.377

After the filtering, the contribution of the geopotential model EGM96 was computed at 1,000 m altitude and removed from the gravity gradient data. The relevant statistics is shown in Table 1, row 3. From this statistics it is clear that the removal of EGM96 contribution did not change significantly the std of the data.

The RTM reduction was applied in order to smooth further the gravity gradient data. The RTM effect was computed for each component at 1,000 m altitude based on the detailed elevation model mentioned previously. The statistics of the RTM reduced values is shown in Table 1, row 4. The RTM reduction did not cause any further smoothing of the data as it is shown from the statistics of Table 1. In this case the reason must be the fact that in the test area the topography is very smooth varying from east to west.

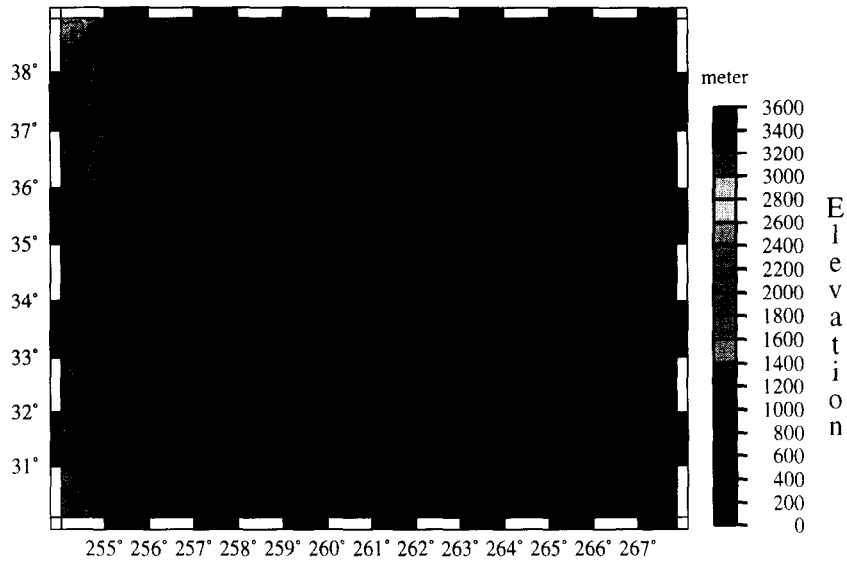

Fig. 1. Oklahoma elevations and distribution of airborne GGSS tracks

For the reasons explained in (Wang, 1988; Arabelos and Tziavos, 1992) a crossover analysis of the data was not attempted. Furthermore, based on the previous experience, only the T_{zz}, T_{xz}, and T_{yz} were used for the prediction experiments, since these components include the main part of the information concerning the gravity field.

In Fig. 4 the T_{zz} field is shown in the test sub-area with the crossing tracks (see Fig. 1) after the removal of EGM96 contribution and the RTM reduction. The main feature in this figure is the wide structure with negative values, oriented from N-E to S-W which is surrounded by steep positive slopes.

Finally, a selection of the data was made, so that one observation per $2' \times 2'$ cell was selected. This selection was based on the filter width used to reduce the noise of the data. After this selection the number of the point data per component was reduced from 44,250 to 1,285.

2.3 Surface gravity data

A 4 km × 4 km point free air gravity anomaly data set was used in the test area (Texas/ Oklahoma). These gravity anomalies are bounded by $33^o \leq \varphi \leq 36^o, 259^o \leq \lambda \leq 264^o$ and originally were given with respect to the gravity formula of GRS67 with all gravity values referred to IGSN71 (Rapp and Zhao, 1988). Then, the gravity anomalies were transformed to GRS80. From the above gravity anomalies the contribution of the EGM96 geopotential model was subtracted and the statistics of the reduced gravity anomalies are given in Table 2 along with the statistics of the observed values. From this table it is shown that the std of the reduced to EGM96 gravity anomalies drops to about 50% of their original std. To smooth further the gravity field, RTM reduction was applied based on the DEM described in section 2.1. The result of this attempt were that the std of the EGM96 reduced gravity anomalies was practically unchanged after the RTM reduction. This is due to the fact that the topography in the test area is rather smoothly varying from west to east.

In Fig. 5 the surface free-air gravity anomaly field is shown after the subtraction of the contribution of the EGM96 and the RTM reduction. The comparison of Figs. 4 and 5 shows the strong correlation of the surface free-air gravity anomaly field with the T_{zz} field at 1,000 m altitude.

Table 2. Statistics of the 4 km × 4 km gridded free-air gravity anomaly data before and after the reductions. Number of observations: 9.608. Unit: mGal.

	Mean	Std	Min. value	Max. value
Δg referred to GRS80	-3.28	24.60	-62.92	78.07
Δg - EGM96	0.83	11.97	-39.38	65.12
Δg - EGM96 - RTM	1.29	11.85	-38.18	65.33

3 Estimation of signal and error covariance functions

In local gravity field modelling using LSC the covariance functions between the involved quantities must reflect the local features of the gravity field and of course they must be compatible in the sense that one should be derivable from the other, according to the covariance propagation low.

The estimation was based on the fitting of the empirical

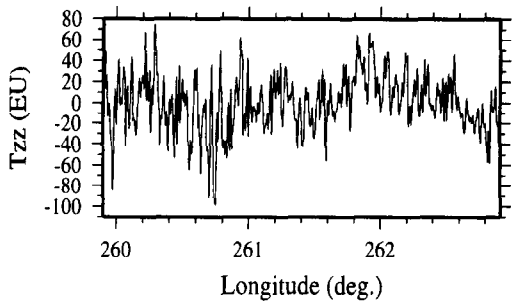

Fig. 2. Original T_{zz} along track No 4

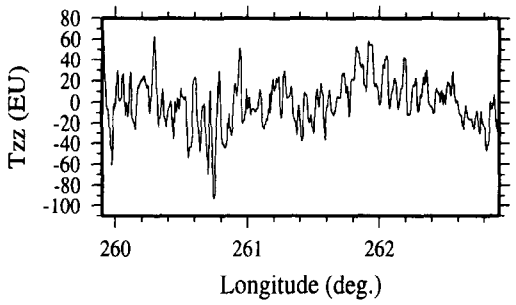

Fig. 3. Filtered T_{zz} along track No 4

covariance values to the analytic expression

$$C(P,Q) = \sum_{i=2}^{360} k\hat{\sigma}_i \left(\frac{R_B^2}{rr'}\right)^{i+2} P_i(cos\psi_{PQ}) + \\ + \sum_{i=361}^{\infty} \frac{A(i-1)}{(i-2)(i+24)} \left(\frac{R_B^2}{rr'}\right)^{i+2} P_i(cos\psi_{PQ}) \qquad (3)$$

In equation (3) r, r' are the distances of the points P, Q from the Earth's centre, $\hat{\sigma}_i$ the error anomaly degree variances (in units of mGal^2) associated with the EGM96 coefficients, k a scale factor, R_B the radius of the so-called Bjerhammar sphere, P_i the Legendre polynomial of degree i, ψ_{PQ} the spherical distance between P and Q, while A is a free parameter in units of mGal^2.

After the estimation of the parameters k, A and R_B of the expression (3), the analytical expression of the covariance function between any other kind of quantities can be computed since this is derived from (3) by applying the covariance propagation law (Tscherning and Rapp, 1974). In this way, the analytical covariance functions for T_{zz}, T_{xz}, T_{yz}, were computed at 1,000 m altitude.

For the computation of the empirical covariance function a subset of the described in section 2.3 data set was used. This subset was bouded by $33.5^o \leq \varphi \leq 36^o, 259.5^o \leq \lambda \leq 263^o$. The std of the EGM96 and RTM reduced gravity

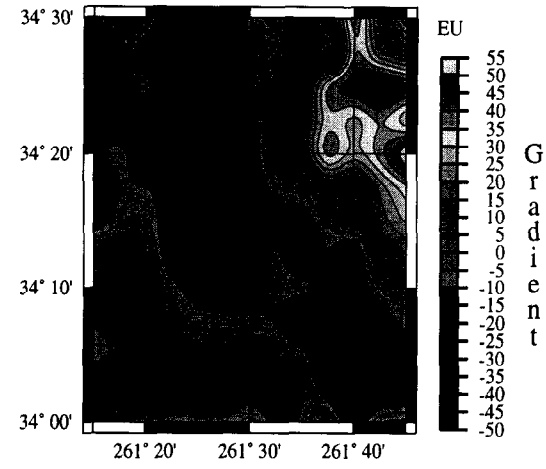

Fig. 4. T_{zz} field in the prediction area after the removal of EGM and RTM contribution

anomalies in this area was equal to 13.4 mGal. The numerical values estimated for the parameters k, A and R_B were 0.037, 180 mGal^2 and -9.758 km respectively. The empirical and the analytical covariance functions are shown in Fig. 6. The std for T_{zz}, T_{xz}, T_{yz}, at 1,000 m altitude according to this local covariance function are 11.75, 8.29 and 8.27 EU respectively. These values are considerably smaller than the actual std of the filtered and reduced to EGM96 corresponding observations (see Table 1).

For the estimation of error covariance functions these analytical covariance functions were compared with corresponding empirical covariance functions computed from the observed airborne gravity gradients. The computation was done in such a way that only data on the same track were used in the estimation. The differences in each case were interpreted as (empirical) error covariance functions. These empirical error covarince functions were modeled as finite error covariance functions using the very simple expression (Sansó and Schuh, 1987, eq. 30):

$$cov(d) = \frac{1}{3}R^6\pi - \frac{1}{2}R^4d^2\pi + \frac{1}{3}\left(R^4d + \frac{4}{3}R^2d^3 - \frac{1}{12}d^5\right) \\ \sqrt{R^2 - \frac{d^2}{4}} + \left(R^4d^2 - \frac{2}{3}R^6\right)\arcsin\left(\frac{d}{2R}\right), \qquad (4)$$

$cov(d) = 0$ for $d \geq 2R$, with R a constant and d the variable distance.

The values to be selected in order to fix the covariance function is the quantity R and a scale-factor so the functions agree with the original one for $d = 0$. R may be selected so that we get the best approximation of the original function, but we chose simply to fix R in order to have the same correlation distance d_1 for the finite and the original function,

$$cov(0)0.5 = cov(d_1) \qquad (5)$$

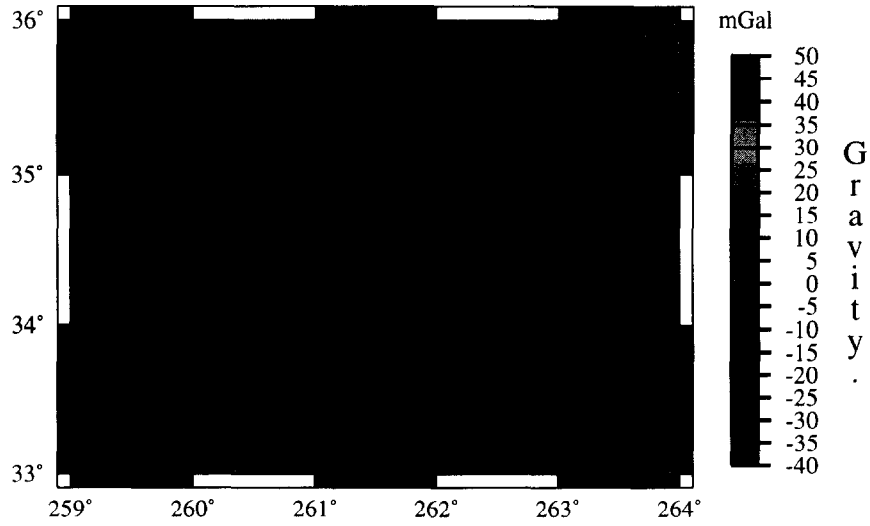

Fig. 5. The free-air gravity anomaly field after removal of EGM96 and RTM contribution

(see also Arabelos and Tscherning, 1998). In Fig. 7 the analytical covariance function of T_{zz} is shown together with the empirical one of T_{zz} and the difference between them.

Although T_{zz}, T_{xz}, T_{yz}, were produced from the same system and filtered using the same filter, the error covariance functions estimated are considerably different (see Table 4) columns 2 and 3 for the parameters of the analytical (finite) error covariance functions). This fact is not easy to be explained. A possible reason could be that resonance effects were acting in a different way on each component during the aircraft flight.

4 Prediction of gravity anomalies from gravity gradient data

Since the target of this work is to study the improvement of the prediction quality when the correlation of the errors is taken into account, the experiments are restricted only in the area with the crossing tracks ($33.75^o \leq \varphi \leq 34.75^o, 261^o \leq \lambda \leq 262^o$). Using gravity gradient data from this area, gravity anomalies were predicted at ground level, in an inner zone ($34^o \leq \varphi \leq 34.30^o, 261.15^o \leq \lambda \leq 261.45^o$). The predicted gravity anomalies were compared to observed values at 160 ground stations. The quality of the prediction is expressed in terms of the mean value and the std of the differences between observed and predicted gravity anomalies.

The empirical auto and cross-covariance functions of all quantities were estimated. However, only the covariance function of gravity anomalies was used to estimate an analytic representation.

In a first stage the prediction was made assuming uncorrelated errors. As data noise the $\sqrt{cov(0)}$ where cov(0) the

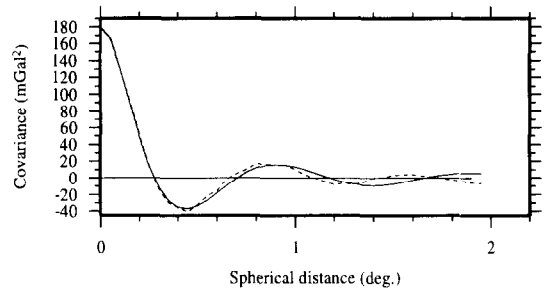

Fig. 6. Covariance function of free-air gravity anomalies (dash line: empirical, solid line: analytical)

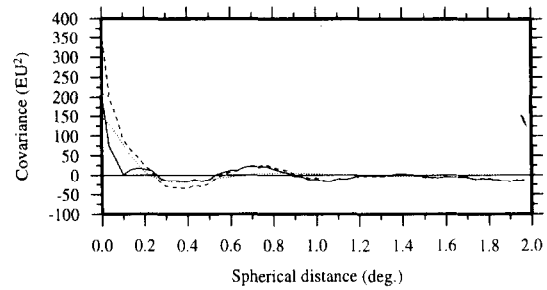

Fig. 7. Empirical covariance function of T_{zz} at 1,000 m altitude (dashed line), the corresponding analytical from free-air gravity anomalies (covariance propagation +upward continuation) (dot line) and their difference (solid line)

variance of the error covariance function of the corresponding quantity was adopted. Numerical experiments showed that these values of data noise resulted in the better prediction results in terms of the mean value and std of the differences between observed and predicted gravity anomalies. The results of this first stage are summarized in Table 3.

Table 3. Results of the prediction of gravity anomalies at zero level from gravity gradient data at 1,000 m altitude, in the test sub-area. The errors considered uncorrelated. 160 control points were used with a mean value equal to 0.13 and std equal to 16.84 mGal

		Observed	- predicted
	Data noise	Mean	Std
Input data	(EU)	(mGal)	(mGal)
T_{zz}	13.4	3.91	5.05
T_{xz}	8.0	6.92	7.41
T_{yz}	14.8	2.83	5.69
T_{zz}+T_{xz}+T_{yz}		4.88	4.54
T_{zz}+T_{xz}+T_{yz}+Δg^*		0.25	3.78

*three surface gravity values

From the statistics of Table 3 it is seen that T_{zz} gives better results than T_{xz} or T_{yz} at least in terms of the std of the differences between observed and predicted values. The combination of the three components gives, as it was expected, even better results than T_{zz}. There is only the problem that the predicted gravity anomalies are considerably biased. This bias is due to the fact that LSC utilizes norm-minimization to fix the so called null-space. The problem is solved by using a small number of surface gravity anomalies as input data. To prove this, three surface gravity values were added to the input data T_{zz} + T_{xz} + T_{yz}. The result was a significant improvement since the mean value of the differences in this case was decreased from 4.88 to 0.25 mGal.

Table 4. Results of the prediction of gravity anomalies at zero level from gravity gradient data at 1,000 m altitude, taking into account correlated errors. The error covariance functions were computed as finite ones from two parameters (variance and half distance to the first zero point). 160 control points were used with a mean value equal to 0.13 and std equal to 16.84 mGal.

	Param. of the	covar. funct.	Obs.	- pred.
		Half dist. to 1st zero		
	Variance	point	Mean	Std
Input data	(EU^2)	(Degree)	(mGal)	(mGal)
T_{zz}	180	0.05	2.71	4.95
T_{xz}	64	0.07	5.41	5.49
T_{yz}	220	0.02	1.90	5.09
T_{zz}+T_{xz}+T_{yz}			2.92	3.96
T_{zz}+T_{xz}+T_{yz}+ +Δg^*			-0.60	3.39

*three surface gravity values

The next stage was to repeat the prediction experiments at the same points and using the same data, but taking into account the error covariance functions computed according to the procedure described in section 3. The predicted gravity anomalies were compared to the same set of observed gravity data as in the first stage. The corresponding statistics is shown in Table 4 together with the parameters of the finite error covariance function used for each component.

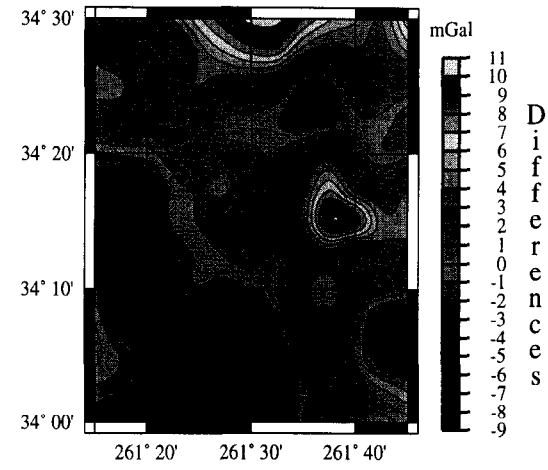

Fig. 8. Differences between observed and predicted gravity anomalies

Comparing the results of Tables 3 and 4 it is clear that the quality of the prediction in all cases is better when the correlated errors are taken into account.

The differences between observed and predicted from the combination (T_{zz}+T_{xz}+T_{yz}+Δg) when correlated errors were considered free-air gravity anomalies are shown in Fig. 8. Taking into account that the std of the observed gravity data is 16.84 mGal and the accuracy of the data is estimated between 2 and 3 mGal, the prediction results of Table 4 could be considered as very satisfactory.

5 Conclusions

The goal of this study was (a) to show how error covariances could be determined and (b) to demonstate numerically the importance of taking correlated errors into account when LSC is used in gravity field modelling. For this purpose, gravity gradient observations were used, assuming that these observations are affected by correlated errors.

The analysis of the gravity gradient observations showed that these data were very noisy. The noise was reduced after a low-pass filtering.

The correlated errors of the gravity gradient data were expressed as error covariance functions. The estimation of these error covariance functions was based on the comparison of empirical signal covariance functions of the gravity gradient data with corresponding signal covariance functions derived from surface gravity anomalies. The errors of the gravity anomalies were assumed uncorrelated. The estimated error covariance functions are significantly different for the various components, although all these components are produced

by the same system. This can be explained if detail information about the measuring system is provided.

The comparison of the predicted gravity anomalies with observed point free-air gravity anomalies showed that in any case the quality of the prediction is better when the error covariance functions are used instead of uncorrelated noise.

The results of the prediction are considered as very satisfactory since more than 80% of the gravity signal was recovered from the combination of $T_{zz}+T_{xz}+T_{yz}$.

A further improvement is possible if error correlations between the different components are estimated and accounted for when using LSC.

References

Arabelos, D., and C.C. Tscherning, Simulation of regional gravity field recovery from satellite gravity gradiometer data using collocation and FFT, *Bull. Geod.*, *64*, 363–382, 1990.

Arabelos, D. and I. N. Tziavos, Gravity field Approximation Using Airborne Gravity Gradiometer data. *J. Geophys. Res.*, *97(B5)*, 7097–7108, 1992.

Arabelos, D. and C.C. Tscherning, The use of least suqares collocation method in global gravity field modeling. *Phys.Chem. Earth*, *.23*, 1–12, 1998.

Brzezowski, S.J., and W. Heller, Gravity gradiometer survey errors, *Geophysics*, *53*, (10), 1355–1361, 1988a.

Brzezowski, S.J., S. D. Gleason, J. Goldstein, W. Heller, C. Jekeli, and J. White, Synopsis of earth field test results from the gravity gradiometer survey system, In Chapman Conference on Progress in the Determination of the Earth's Gravity Field, Fort Lauterdale, Florida, 1988b.

Forsberg, R. and C.C. Tscherning, The use of height data information in gravity field approximation by collocation. *J. Geophys. Res.*, *86(B9)*, 7843–7854, 1981.

Gleason, D.M., An initial look at 54 tracks of airborne data from the gravity gradiometer data, In Proc. of the 16th Annual Gravity Gradiometer Conference, Colorado Springs, Colorado, 1988.

Jekeli, C., On optimal estimation of gravity from gravity gradient at aircraft altitude, *Rev. Geophys.*, *19*, 213–221, 1985.

Lemoine, F.G. et al., 1996. The Developement of the NASA GSFC and NIMA Joint Geopotential Model. Proceedings GRAGEOMAR, Tokyo, Sept.30 -Oct. 5.

Moritz, H. Advanced physical Geodesy, Herbert Wichmann Verlang Karlsruhe, 1980.

Rapp, R.H., and S. Zhao, The 4 km×4 km free-air anomaly file for the continental United States, Internal Rep., Dep. of Geod. Sci. and Surv., Ohio State Univ., Columbus, 1988.

Sansó, F., W.-D.Schuh: Finite Covariance Functions. *Bull. Geod. 61*, 331–347, 1987.

Tscherning, C.C, and R.H. Rapp, Closed covariance expressions for gravity anomalies, geoid undulations and deflections of the vertical implied by anomaly degree variance models. Dept. of Geodetic Science, Report No. 208, The Ohio State University, 1974.

Tscherning, C.C., GEOCOL-A FORTRAN-program for gravity field approximation by collocation, Technical Note, Geodaetisk Institut, 12th edn., 1997.

Vasco, D.W., Resolution and variance operators of gravity and gravity gradiometry, *Geophysics*, *54* (7), 889–899, 1989.

Wang, Y. M., Determination of the gravity disturbance on the earth's topographic surface from airborne gravity gradient data, Rep. 401, Dep. of Geod. Sci. and Surv., Ohio State Univ., Columbus, 1988.

Wessel, P., and W.H.F. Smith, New version of the Generic Mapping Tools (GMT) released, *EOS Trans. AGU*, *76*, p. 329, 1995.